P9.2 A simple-but-realistic fuzzy logic hydrometeor classification scheme for the French X, C and S-band polarimetric radar

Hassan AL-SAKKA*, F. Kabeche, J. Figueras i Ventura, B. Fradon, A. A. Boumahmoud, and P. Tabary.
Météo France, Toulouse, France

1. INTRODUCTION

The ability to perform hydrometeor classification at high space-time resolution (5 minutes – 1 km²) in precipitating systems is one of the main benefits brought by polarimetry. Polarimetric Radar measurements of precipitation vary with the hydrometeor properties such as the shape, the size, the orientation, the phase state and the fall rate.

For the classification of hydrometeor in Météo France, we use the fuzzy logic hydrometeor classification scheme presented by Marzano et al., (2006). We revisit it with the aim to make it more realistic (with respect to actual radar measurements), simpler and more efficient compared to previous approaches.

The paper is structured as follows: Section 2 provides an overview of the current scheme of classification, Section 3 introduces the membership functions with their dependence on actual measurement conditions, Section 4 analyses the preliminary results obtained by the algorithm, while conclusions are discussed in section 5.

2. FUZZY LOGIC CLASSIFICATION METHOD

A non linear method, it is one of the best solutions for the hydrometeor classification, see Bringi and Chandrasekar (2001) and Zrnic et al. (2001). The input data vectors are the reflectivity Z_H, the differential reflectivity Z_{DR}, the specific differential phase K_{DP}, the co-polar correlation coefficient ρ_{HV} and the temperature T. The output data is the precipitation type of each pixel.

As a first step, in our study and for this method, we define the number of hydrometeor types as 5 : Rain (RA), Wet Snow (WS) or melting snow, Dry Snow (DS), Ice (I) or crystals and Hail (HA). In future work, the case of HA must be extended to 3 types : small Hail (diameter < 5 mm), medium Hail (diameter between 5 – 20 mm) and large Hail (diameter > 20 mm). Adding more hydrometeor types at this stage would not be realistically compatible with the known discriminating power of the polarimetric variables collected operationally.

The second step consists of establishing empirical 2D membership functions (2DMBF) for (Z_H, Z_{DR}), (Z_H, K_{DP}) and (Z_H, ρ_{HV}) in so-called “ideal conditions”. More details about the 2DMBR are in the next section.

We can summarize the method as follows: for each polar pixel, the actual measurement conditions are taken into account to generate modified 2DMBF from the ideal 2DMBF. The resulting modified 2DMBF values for (Z_H, Z_{DR}), (Z_H, K_{DP}) and (Z_H, ρ_{HV}) are calculated and added for each hydrometeor type. We add a probability function called bright band function, its role is to promote a type from another. More details on this function are in the next section. The result is multiplied by a 1D temperature-dependent MBF. The hydrometeor with the highest score (or highest probability, maximum probability function) is considered as the dominant one. Equation 1 resumes the calculation of the score, the probability function :

$$P_F^i = F_Z^i(Z_H)\,F_T^i(T)[F(Z_H,Z_{DR}) + F(Z_H,K_{DP}) + F(Z_H,\rho_{HV}) + F_{BB}^i(BB)] \quad (1)$$

Different probability functions exist in the various works, see Lim et al. (2005) and Keenan, 2003. The main difference with our probability function is that our function does not use the weight factors of the polarimetric parameters and it is unique for the C, S, X-band radar.

3. THE MEMBERSHIP FUNCTIONS

A membership function 1D is a trapezoidal function of probability values, see Zrnic et al. (2001) or a beta function, see Liu and Chandrasekar (2000). The 2DMBF is a domain of probability for each couple of polarimetric variables in the Z_H and other parameter (Z_{DR}, K_{DP}, ρ_{HV}) plan. The membership functions are segregated by hydrometeor type and by wavelength (S, C and X-band).

The steps to establish these functions are : 1) chose the data in so-called “ideal conditions”. “Ideal conditions” refers here to low attenuation (Φ_{DP} < 10°), high Signal-to-

* *Corresponding author address :* Hassan AL-SAKKA, Météo France, DSO/CMR/DEP, 42 Av. Coriolis, 31057 Toulouse, France ; +33 567698792 ; e-mail :hassan.al-sakka@meteo.fr

Clutter Ratio (SCR > 10 dB), high Signal-to-Noise Ratio (SNR > 20 dB), low Partial Beam Blocking (PBB < 10%) and short distances (d < 60 km). A large number of radar data collected by the French polarimetric radars (9 C-band, 1 S-band, 1 X-band) are used in that step and areas of homogeneous hydrometeor types are determined subjectively by an expert. This constitutes the calibration and validation dataset. 2) projected the couple of polarimetric parameters, i.e. (Z_H, Z_{DR}), in its corresponding plan. 3) modeled the 2DMBF by using two half-Gaussians (an upper one and a lower one) per class of Z_H (5 dBZ increment. We choose the two half-Gaussians as function of the model. 4) analyzed and parameterized the dependency of the modeled 2DMBF with the actual measurements conditions (Φ_{DP}, SCR, SNR, PBB, distance, …).

The two half-Gaussians function is more realistic, more reliable and less parameters than a Gaussian or a trapezoidal function as in Zrnic et al. (2001) especially for the membership functions of (Z_H, ρ_{HV}) because the widths are not the same on each side.

Each two half-Gaussians function is characterized by 3 parameters : the position of the maximum and the 2 half-width from the left W_1, and from the right W_2 of the maximum position, they represent the standard deviations of this function.

3.1 Calculation of the dependency of 2DMBF with the actual measurement conditions

To analyze and parameterize the dependency of the modeled 2DMBF with the actual measurement conditions, we start by calculating the widths of the two half-Gaussians functions in so-called "ideal conditions" as we mentioned above. As we change 1 condition (i.e. $10° < \Phi_{DP} < 30°$), we measure the impact of this variation on the width. We assume that the variations (enlargements widths) are linear with the variations of the measurement conditions. We also assume that the enlargement widths are the same for all types of precipitation, i.e. the enlargement of the 2DMBF (Z_H, Z_{DR}) of the Hail type is the same for the Wet Snow type for a given radar wavelength. Tables 1-3 resume the variation rate of the 2DMBF C, S and X-band radar. A : is the variation of SCR from [0,10] to [10,30] with an attenuation ($\Phi_{DP} < 10°$). B : is the variation of the attenuation from [0,10] to [10,30] with a SCR between [10,30]. C : is the variation of the attenuation from [0,10] to [10,30] with a SCR between [0,10].

X-band	Z-Z_{DR}		Z-K_{DP}		Z-ρ_{HV}	
	W_1	W_2	W_1	W_2	W_1	W_2
A	39.7	10.9	14.9	16.7	15.6	8.9
B	34.7	12.6	16.7	28.4	35.6	8.3
C	38.9	14.4	8.4	25.1	64.9	8.2

Table. 1 The variation rate (the enlargement) of the two half-Gaussians function widths in X-band.

S-band	Z-Z_{DR}		Z-K_{DP}		Z-ρ_{HV}	
	W_1	W_2	W_1	W_2	W_1	W_2
A	1.0	1.0	1.0	1.0	1.0	1.0
B	35.6	27.5	14.3	4.8	8.4	5.6
C	62.4	45.6	14.3	15.9	8.4	5.6

Table. 2 The variation rate (the enlargement) of the two half-Gaussians function widths in S-band.

C-band	Z-Z_{DR}		Z-K_{DP}		Z-ρ_{HV}	
	W_1	W_2	W_1	W_2	W_1	W_2
A	30.6	12.2	15.0	1.0	34.3	1.0
B	19.5	10.1	11.3	13.5	15.5	1.0
C	7.5	27.3	6.9	20.2	16.3	1.0

Table. 3 The variation rate (the enlargement) of the two half-Gaussians function widths in C-band.

Note that The Partial Beam Blocking PBB did not affect the membership functions.

3.2 Bright Band Functions

The Bright Band (BB) is the altitude level where the temperature is 0°C. In this altitude, snow is formed. The dual-polarization processing chain of Météo France can detect the bright band, see Tabary et al. (2006) for more details.

The BB functions are used in the probability function as an additive term to promote one type from another. There are 3 types of these functions: 1) under BB where the Rain is promoted. 2) in BB where Wet Snow is promoted. 3) above BB where Dry Snow and Ice are promoted. Hail can be presented in any altitude so the BB does not affect the presence of the Hail.

The main inconvenience of the BB is the difficulty of its detection.

The BB functions are the same for all radar wavelengths.

3.3 Temperature function

The temperature function is the most important function in the algorithm of hydrometeor classification. According to equation 1, it is a multiplicative function. For example when the temperature is more than 3℃, we can not have any type of Snow. Table 4 resumes the value of the temperature domain of each hydrometeor type.

Temp (℃)	X1	X2	X3	X4
RAIN	-4	0.5	50	50
WETSNOW	-5	-2	5	10
DRYSNOW	-60	-50	0	3
ICE	-75	-70	-10	-3
HAIL	-90	-20	20	40

Table 4 The trapezoid parameters, see Snyder et al. 2010, of the temperature function.

For this reason, a good detectability of temperature along with the radar beam allows a better classification.

In the actual dual-polarization processing chain of Météo France, the temperature is estimated using the bright band detection algorithm. At this level, the temperature is 0℃. For the temperature profile, we apply the -6.5℃/Km profile expression.

In an ideal case, this method would work well, but the problem is when a cold front approaches the zone detected by the radar, the detection of the temperature is analyzed incorrectly.

The temperature functions are the same for all radar wavelength.

Different approaches exist to replace the temperature detectability : a 3D temperature field model, this model comes from a mix of observations at different altitude levels and simulations. It can provide values every hour but the time of computation takes longer. Another approach is based on the prevision temperature data.

The main goal is to apply one of these approaches in real time. This issue will be analyzed soon to answer our needs taking into account the required constraints.

3.4 T-matrix simulation

It is a simulation method to calculate the result of the scattering of the electromagnetic waves by particles, see Barber and Hill (1990). It has been modified to obtain the polarimetric signature and their relation with hydrometeor properties by Mishchenko and his team, see Mishchenko et al. (1996) and Mishchenko and Travis (1998).

We use this method to enhance our membership function as we can see in figure 1. The “black stars” line represents the result of the simulation using T-matrix. This curve helps us to extrapolate the MBF when the number of pixels is not enough or the values of Z_H and Z_{DR}, for example, are dispersed as we can see in figure 1 when the values of Z_H are more than 45 dB. The parameterization of the T-matrix algorithm are the same as Ryzhkov and Zrnic (2005) and Gourley et al. (2008).

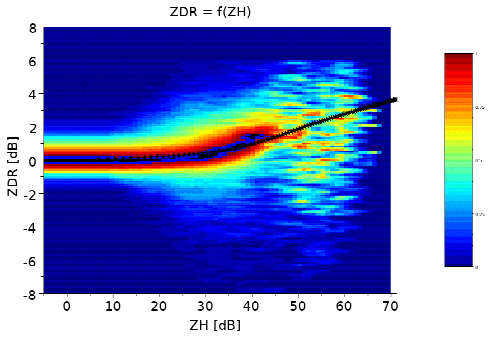

Fig. 1 Example of the Z_H-Z_{DR} membership function at X-band using real data with a matching curve using T-matrix simulation.

4. RESULTS AND DISCUSSIONS

To establish the membership functions, we used different radars at C, X and S-band within a 4 day range. We use one elevation, the lowest possible without significant impact of partial beam blocking.

Our objective was to have a unique algorithm, with membership functions for each radar band, which take into account the measurement conditions.

The first result, figure 5 , is a examples of hydrometeor classification with PPI of the Z_H, Z_{DR}, ρ_{HV}, figures 2 to 4, Cherves Radar (C-band), Météo France, 2010/11/14, 1° of elevation. The two black concentric circles in each figure (2 to 6) represent the Bright band.

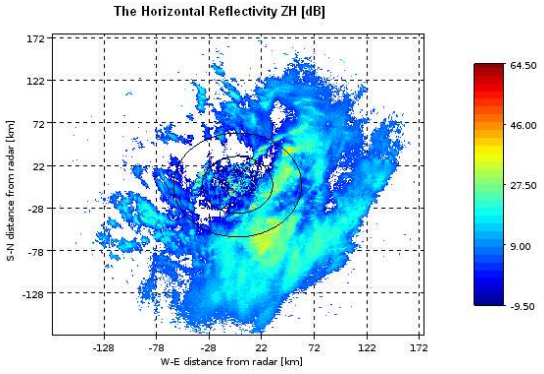

Fig. 2 Example of a Z_H PPI, Cherves Radar (C-band), Météo France, 2010/11/14, 12:00, 1° of elevation. The 2 concentric circles represent the Bright band.

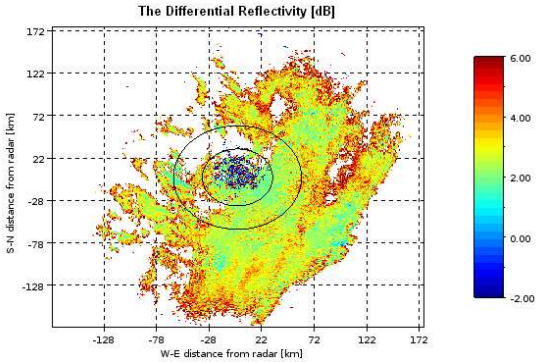

Fig. 3 Example of a Z_{DR} PPI, Cherves Radar (C-band), Météo France, 2010/11/14, 12:00, 1° of elevation.

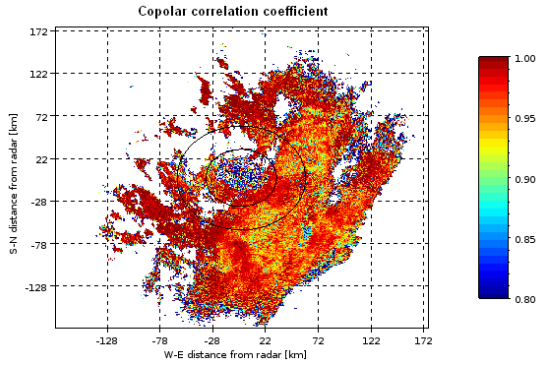

Fig. 4 Example of a ρ_{HV} PPI, Cherves Radar (C-band), Météo France, 2010/11/14, 12:00, 1° of elevation.

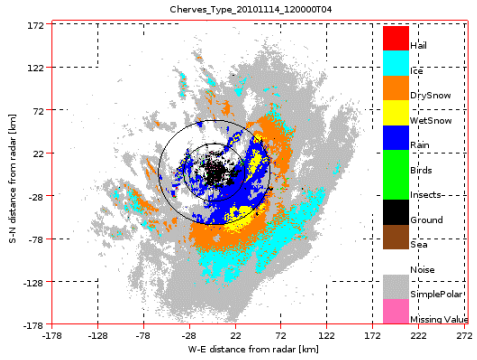

Fig. 5 Example of the classification using the new approach of classification, Cherves Radar (C-band), Météo France, 2010/11/14, 12:00, 1° of elevation.

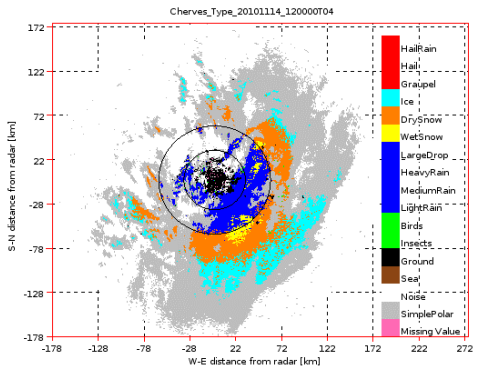

Fig. 6 Example of the classification using the old approach of classification, Cherves Radar (C-band), Météo France, 2010/11/14, 12:00, 1° of elevation.

An analysis to have a comparison between the old and the new algorithm. Figure 5, shows a case where we used the new approach of the classification. By comparing with the old classification, figure 6, we can remark an improvement of the detection of Wet Snow without using weight as explained before. We can also remark more homogeneity for each type of precipitation.

In the second part of the analysis, we computed the second choice in the algorithm, i.e. the second hydrometeor type which probability function is the second in descending order. In our view, this study brings more consistence of the results when the difference between the first and the second choice is significantly high (more than 25%). Figure 7 shows the difference for 1 day of results, Cherves Radar (C-band), Météo France, 2010/11/14, 1° of elevation and the figure 8 represents the number of pixels corresponding to each type of precipitation in figure 7. We can remark that the choice of Rain type is significantly improved by the percentage of difference (40% in average) between the first and the second choice. The Hail detection remains difficult due to the low number of pixels classifying Hail and the common areas between the membership function of Hail and Rain (the signature of the large Drop).

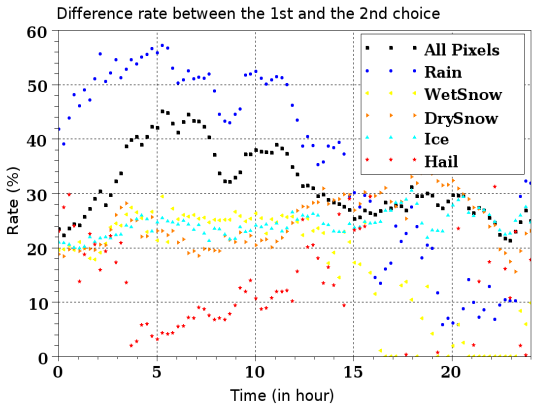

Fig. 7 Example of the computation of the difference between the first and the second choice of the hydrometeor classification algorithm for one day of measurements, Cherves Radar (C-band), Météo France, 2010/11/14, 1° of elevation.

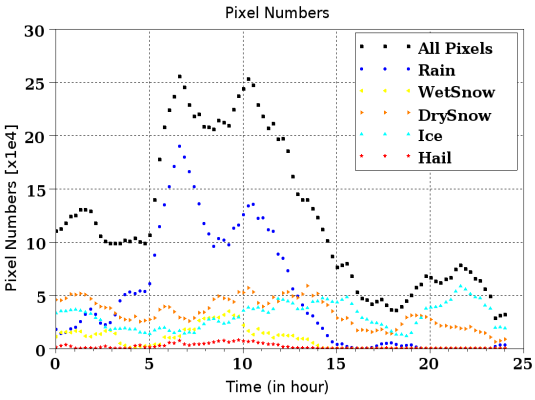

Fig. 8 The corresponding number of pixels used in figure 7, Cherves Radar (C-band), Météo France, 2010/11/14, 1°of elevation.

For Wet Snow, Dry Snow and Ice, the difference rates are “acceptable” but more analysis is needed to improve these classifications.

Qualitative study is intended to compute the scores of each types by comparing with other algorithms of hydrometeor classification.

5. CONCLUSION

This paper has provided an overview of the hydrometeor classification algorithm, especially the corresponding membership function of each type, the bright band and the temperature functions.

One can say that the enlargement of the weights of the MBF gives to the study more reality and more flexibility. T-matrix simulation enhances the MBF computed using real data from operational radar network as the Météo France Radar network.

Using one probability function reduces the number of parameters and the idea of having one algorithm for the C, S and X-band radar is more powerful than having an algorithm for each radar band.

More studies are planned to improve the detection of the temperature along the radar beam by using different techniques as we mentioned above. But we must always take into account the time of computing to achieve our goal : have a real time hydrometeor classification product.

The difference between the old and the new algorithm is that we can use a simple and more realistic algorithm, unique for the radar bands, while maintaining an important level of classification success.

The study of the difference between the first and the second choice of the hydrometeor classification algorithm shows the capacity of the algorithm to separate two hydrometeor types, especially when the common area of MBF is scientifically large.

A study of the Hail is also planned to extend it to 3 types : small Hail (diameter < 5 mm), medium Hail (diameter between 5 – 20 mm) and large Hail (diameter > 20 mm). This study should enrich our algorithm and, with real time production, enhance the prevention of the risks due to medium and large Hail.

REFERENCES

Bringi, V. N., and V. Chandrasekar, 2001: Polarimetric Doppler Weather Radar: Principles and Applications. *Cambridge University Press*, 636 pp.

Gourley, JJ., A.J. Illingworth and P. Tabary, 2008 : Absolute calibration of radar reflectivity using redundancy of the polarization observations and implied constraints on drop shapes, *J. Atmos. Oceanic Technol.*

Keenan, T., 2003: Hydrometeor classification with C-band polarimetric radar. *Aust. Meteor. Mag*., 51, 23-31.

Lim, S., V. Chandrasekar, and V. N. Bringi, 2005: Hydrometeor classification system using dual polarization radar measurements: Model improvements and in situ verification. *IEEE Trans. Geosci. Remote Sens*., 43, 792–801.

Liu, H., and V. Chandrasekar, 2000: Classification of hydrometeors based on polarimetric radar measurements: Development of fuzzy logic and neuro-fuzzy systems, and in situ verification. *J. Atmos. Oceanic Technol*., 17, 140–164.

Marzano, F. S.,D. Scaranari,M. Celano, P. P.Alberoni, G.Vulpiani, and M.Montopoli, 2006: Hydrometeor classification from dualpolarized weather radar: Extending fuzzy logic from S-band to C-band. *Adv. Geosci.*, 7, 109–114.

Mishchenko, M.I., and L.D. Travis, 1998: Capabilities and limitations of a current FORTRAN implementation of the T-matrix method for randomly oriented, rotationally symmetric scatterers. *J. Quant. Spectrosc. Radiat. Transfer*, 60, 309-324.

Mishchenko, M.I., L.D. Travis, and D.W. Mackowski, 1996: T-matrix computations of light scattering by nonspherical particles: A review. *J. Quant. Spectrosc. Radiat. Transfer*, 55, 535-575.

Ryzhkov, A. V., and D. S. Zrnic´, 2005: Radar polarimetry at S, C, and X bands:Comparative analysis and operational implications. *32nd Conf. on Radar Meteorology*, Albequerque, NM. Amer. Meteor. Soc., 9R.3.

Snyder, J. C., H. B. Bluestein, G. Zhang, S. J. Frasier, 2010: Attenuation Correction and Hydrometeor Classification of High Resolution, X-band, Dual-Polarized Mobile Radar Measurements

in Severe Convective Storms, J. Atmos. Ocean. Tech, Accepted.

Tabary, P., A. Henaff, G. Vulpiani, J. Parent-du Chatelet, and J. Gourley, 2006: Melting layer characterization and identification with a C-band dual-polarization radar: A long term analysis. Preprints, Fourth European Conf. on Radar in Meteorology and Hydrology (ERAD 2006), Barcelona, Spain, *Servei Meteorolo` gic de Catalunya,* 17–20.

Zrnic´, D. S., A. V. Ryzhkov, J. Straka, Y. Liu, and J. Vivekanandan, 2001: Testing a procedure for automatic classification of hydrometeor types. *J. Atmos. Oceanic Technol*., 18, 892–913.